(Received 2 January 2025, Accepted 20 January 2025, Scheduled 28 January 2025)

A Novel Wideband Reflectionless Filtering Patch Antenna

Shuai Gao, Zhongbao Wang*, Hongmei Liu, and Shaojun Fang

School of Information Science and Technology, Dalian Maritime University, Dalian, Liaoning 116026, China

ABSTRACT: In this paper, a novel wideband reflectionless filtering patch antenna is proposed. The antenna consists of a filtering patch and an absorption network. The filtering patch includes an E-shaped radiator and two T-shaped radiators. The E-shaped radiator introduces a radiation null, which greatly improves lower-band edge selectivity. The T-shaped radiators introduce an additional radiation null, effectively increasing the filtering performance in the upper stopband. For the absorption network, a quarter-wavelength coupled-line section with two 200-ohm resistors and four short-circuited three-quarter-wavelength transmission lines are used to achieve reflectionless characteristics. To demonstrate the design, an antenna prototype with a center frequency of 3.5 GHz is fabricated and measured. Measurement results manifest that the input reflectionless bandwidth is 63.5% from 2.56 to 4.94 GHz with an antenna gain of 5.8 dBi. At 3.02 and 3.91 GHz, two radiation nulls are also obtained. The lower and upper stopband suppression levels are 18.1 and 14.5 dB, respectively.

1. INTRODUCTION

As 5G technology rapidly evolves, filtering antennas have received increasing attention for their simple structure, low loss, and high performance. Filtering antenna design methods are generally classified into three categories. The first method is to simply cascade antennas and filters [1, 2]. The second method is to use the antenna as the last resonator stage of the bandpass filter, which is realized by coupling matrix theory [3]. The third method is co-designed filtering antenna, such as stacked parasitic patches [4] and shorting pins [5]. Although filtering antennas have solved many problems, and many studies on filtering antennas have been conducted for different design objectives such as high selectivity [6], high gain [7], and low cost [8], the out-of-band reflected waves of traditional filtering antennas will affect the stability of the communication system [9]. So the filtering antennas with the function of absorbing out-of-band reflected wave energy are being gradually designed.

Reflectionless filtering patch antennas [10, 11] are a new type of antenna that can transmit or receive the desired signal in the operating band and suppress the undesirable signal outside the band. It effectively solves the effect of signals reflected from the stopband when the antenna is connected to a power amplifier. Currently, the dominant method for reflectionless filtering antenna design is to apply the notion of frequency complementary duplexing [11], so that an antenna and a band-stop filter operate at the same frequency but with opposite responses. For example, a band-stop filter loaded with a resistor is connected in parallel with the feeding line of the antenna [12, 13]. However, the mentioned reflectionless filtering antennas do not achieve particularly wide reflectionless bandwidths, which means that their application scenarios have limitations.

This paper presents a novel wideband reflectionless filtering patch antenna. Its filtering antenna section produces two radiation nulls, resulting in good filtering performance. The wideband reflectionless characteristic is achieved by using an absorption network, which consists of a quarter-wavelength coupled-line section, two 200-ohm resistors, and four short-circuited three-quarter-wavelength transmission lines. The reflectionless filtering patch antenna is simulated by Ansys High Frequency Structure Simulator (HFSS). The results show that it obtains wideband reflectionless characteristics and good filtering performance.

2. ANTENNA CONFIGURATION

Figures 1(a), 1(b), and 1(c) show the structure of the proposed wideband reflectionless filtering patch antenna. The antenna is composed of an F4B substrate (dielectric constant $\varepsilon_r = 2.6$, loss tangent $\tan\delta = 0.003$, thickness $H = 1.5$ mm). On the substrate, the reflectionless filtering patch antenna includes a feeding line, an absorption network, and a filtering patch. The absorption network includes a quarter-wavelength coupled-line section with two 200-ohm resistors and four short-circuited three-quarter-wavelength transmission lines. The filtering patch includes an E-shaped radiator and two T-shaped radiators. Table 1 lists the values of all geometric parameters shown in Fig. 1(b).

TABLE 1. Parameters of the proposed wideband reflectionless filtering patch antenna (Unit: mm).

L_a	8	L_3 ($\approx \lambda/4$)	14.8	W_1	15.7	P_1	1.5
L_b	13.16	L_4	9.25	W_2	4.1	C_1	2
L_c ($\approx \lambda/4$)	12.07	L_5 ($\approx \lambda/2$)	26.65	W_3	2.18	C_2	0.2
L_d ($\approx \lambda/2$)	30.43	W_a	4.1	W_4	8.6	C_3	4
L_e ($\approx 3\lambda/4$)	42.52	W_b	0.91	W_5	10	G_1	110
L_1 ($\approx \lambda/2$)	25.7	W_c	0.77	R_1	0.5	G_2	65
L_2 ($\approx \lambda/4$)	14.3	W_e	2.9	S_1	0.5	H	1.5

* Corresponding author: Zhongbao Wang (wangzb@dlmu.edu.cn).

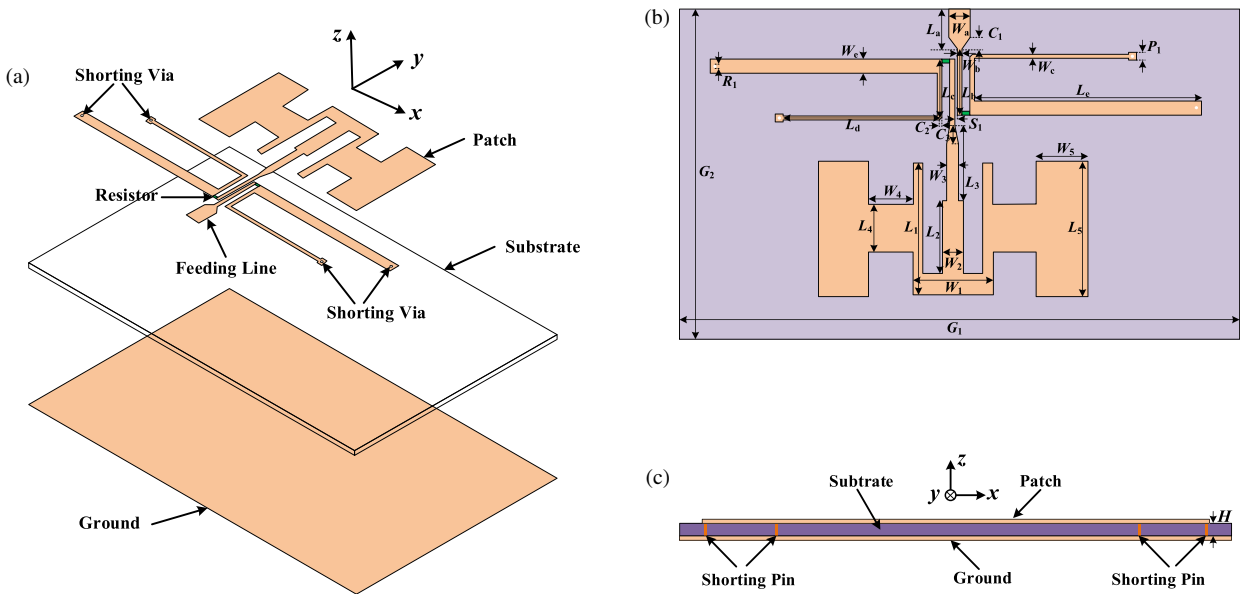

FIGURE 1. Configuration of the proposed reflectionless filtering antenna. (a) Exploded view. (b) Top view. (c) Side view.

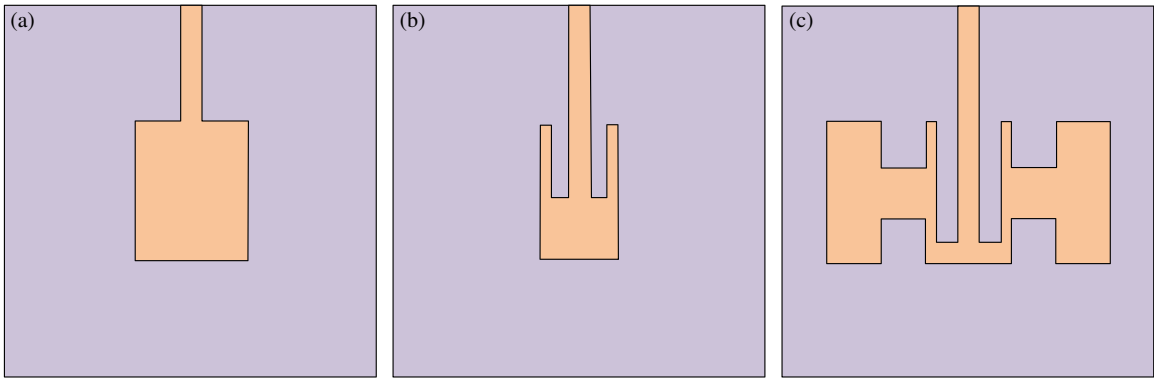

FIGURE 2. Evolution process. (a) Ant. I, (b) Ant. II, (c) Ant. III.

3. ANTENNA ANALYSIS

3.1. Analysis of Filtering Antenna

To better understand the filtering mechanism of the proposed antenna, the development process from Ant. I to Ant. III is shown in Fig. 2, and the curves of the $|S_{11}|$ and realized gains at the direction of the $+z$ axis for each stage of the antenna evolution are given in Figs. 3(a) and 3(b), respectively. Firstly, Ant. I shown in Fig. 2(a) is an ordinary side-feeding rectangular patch antenna without any filtering performance. Then, the rectangular patch is etched with two slots, so Ant. I evolves into Ant. II shown in Fig. 2(b). Ant. II is an E-shaped patch antenna, which successfully generates a radiation null as shown in Fig. 3(b). When T-shaped patches are added on both sides of the E-shaped patch, another radiation null is introduced at 3.74 GHz as shown in Fig. 3(b). Ant. III in Fig. 2(c) is a filtering antenna without out-of-band reflectionless function.

To illustrate exactly how the radiation nulls generate, the simulated current distribution is shown in Figs. 4(a) and 4(b). The main reason for the first radiation null (RN 1) is that the current flow on the middle branch of the E-shaped radiator is reversed from the current flow on the two side branches of the E-shaped radiator as shown in Fig. 4(a), resulting in their radiation fields canceling out in the far field. For the second radiation null (RN 2), the current distribution is shown in Fig. 4(b). We can see multiple current reversals in the branches of the T-shaped radiator and the branches of the E-shaped radiator, which results in the energy not being radiated normally. As a result, another radiation null is generated.

3.2. Analysis of Absorption Network

Figure 5(a) illustrates the equivalent circuit of the absorption network, which consists of a section of $\lambda/4$ coupled lines, two absorption resistors ($R = 200\,\Omega$), and two short-circuited $3\lambda/4$ transmission lines with the characteristic impedances of Z_{TL} and the electrical length of $\theta_{\mathrm{TL}} = 270°$. The coupled lines with the electrical length of $\theta = 90°$ have even- and odd-mode

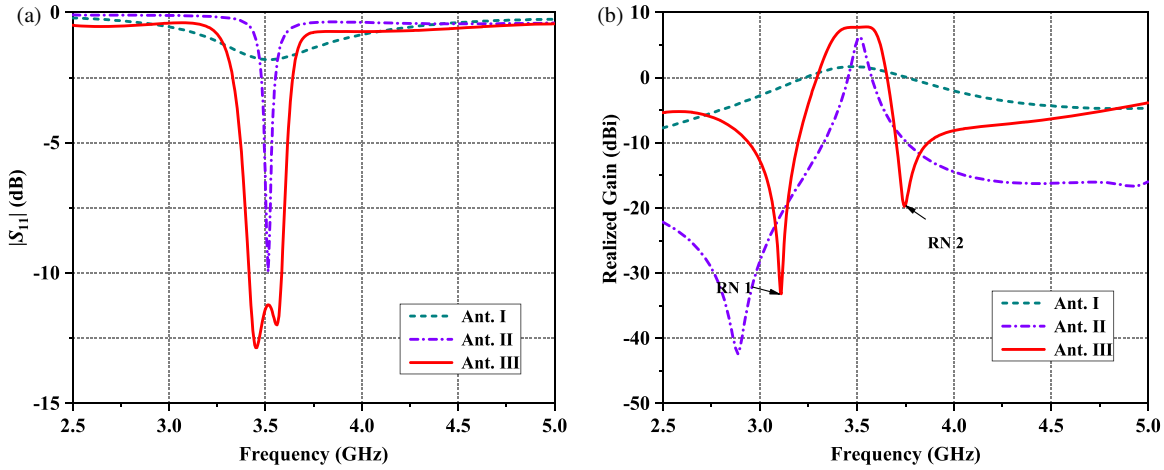

FIGURE 3. Comparisons of (a) simulated $|S_{11}|$ and (b) realized gain.

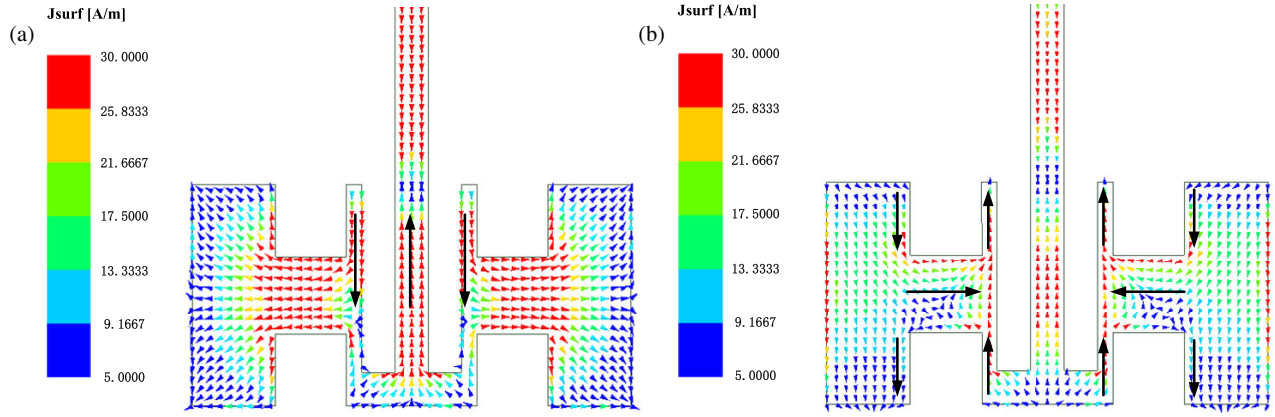

FIGURE 4. Current distributions of the filtering antenna at (a) 3.10 GHz and (b) 3.74 GHz.

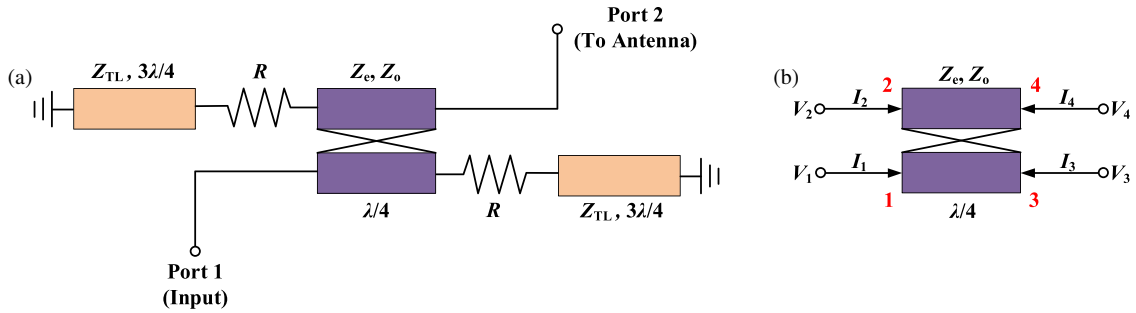

FIGURE 5. (a) Equivalent circuit of the absorption network. (b) Coupled-line network.

characteristic impedances of Z_e and Z_o, respectively. Port 2 is connected to the antenna with a port impedance of $Z_0 = 50\,\Omega$.

As shown in Fig. 5(b), according to network theory, the voltage-current relationship of each port of the coupled lines is as follows:

$$V_1 = Z_{11}I_1 + Z_{12}I_2 + Z_{13}I_3 + Z_{14}I_4 \quad (1)$$

$$V_2 = Z_{21}I_1 + Z_{22}I_2 + Z_{23}I_3 + Z_{24}I_4 \quad (2)$$

$$V_3 = Z_{31}I_1 + Z_{32}I_2 + Z_{33}I_3 + Z_{34}I_4 \quad (3)$$

$$V_4 = Z_{41}I_1 + Z_{42}I_2 + Z_{43}I_3 + Z_{44}I_4 \quad (4)$$

$$V_2 = V_3 = -\left(R + \mathrm{j}Z_{\mathrm{TL}}\tan\theta_{\mathrm{TL}}\right)I_2 \quad (5)$$

$$\begin{cases} Z_{11} = Z_{22} = Z_{33} = Z_{44} = -\mathrm{j}\frac{Z_e+Z_o}{2}\cot\theta = Z_1 \\ Z_{12} = Z_{21} = Z_{34} = Z_{43} = -\mathrm{j}\frac{Z_e-Z_o}{2}\cot\theta = Z_2 \\ Z_{13} = Z_{31} = Z_{24} = Z_{42} = -\mathrm{j}\frac{Z_e-Z_o}{2}\csc\theta = Z_3 \\ Z_{14} = Z_{41} = Z_{23} = Z_{32} = -\mathrm{j}\frac{Z_e+Z_o}{2}\csc\theta = Z_4 \end{cases} \quad (6)$$

Through Equations (1)–(6), the A-matrix of the equivalent circuit can be calculated as

$$[A] = \begin{bmatrix} A_{11} & A_{12} \\ A_{21} & A_{22} \end{bmatrix} \quad (7)$$

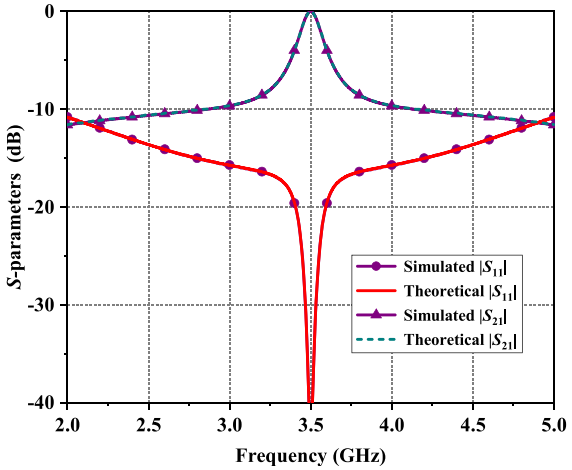

FIGURE 6. Simulation and theoretical calculation S-parameters of the absorption network with $Z_e = 153.8\,\Omega$, $Z_o = 54.5\,\Omega$, and $Z_{\rm TL} = 31.5\,\Omega$.

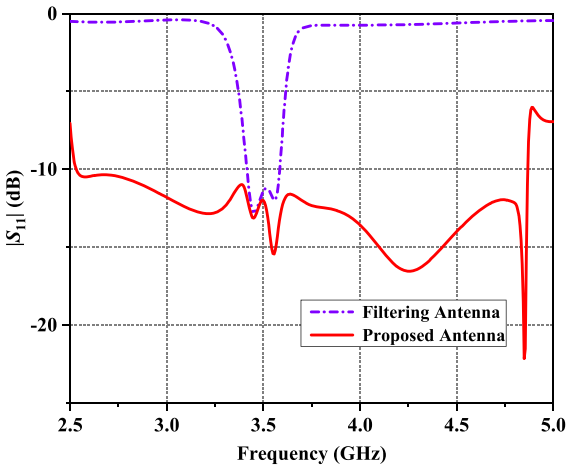

FIGURE 7. $|S_{11}|$ of the filtering antenna and the proposed antenna.

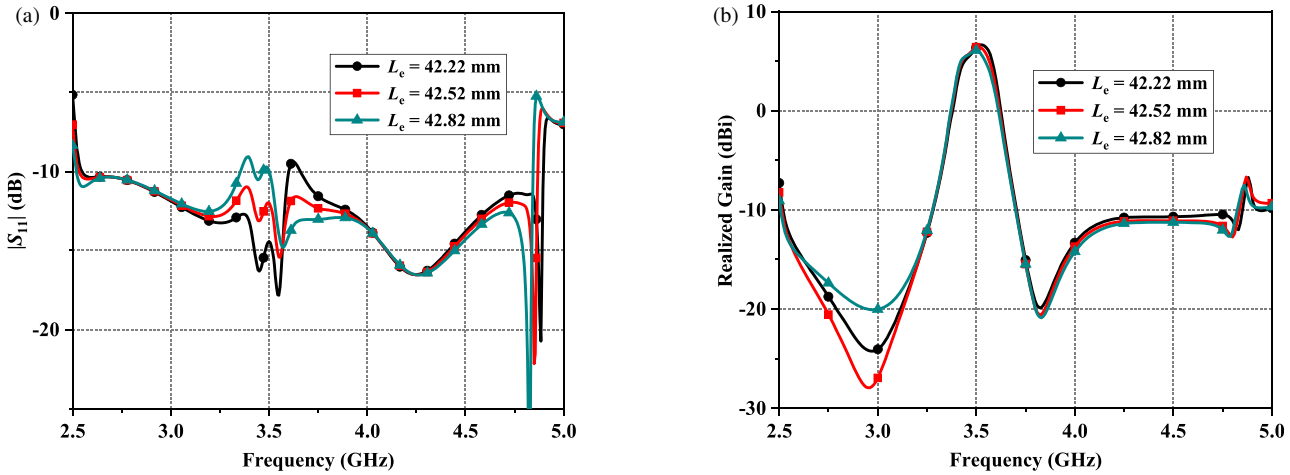

FIGURE 8. Effect of L_e on the performances of the proposed antenna. (a) $|S_{11}|$. (b) Realized gain.

where

$$\begin{cases} A_{11} = \frac{Z_1+Z_3B-Z_2D}{Z_4+Z_2B-Z_3D} \\ A_{12} = \frac{(Z_1+Z_3B-Z_2D)(Z_1+Z_2C-Z_3E)}{Z_4+Z_2B-Z_3D} \\ \qquad -(Z_4+Z_3C-Z_2E) \\ A_{21} = \frac{1}{Z_4+Z_2B-Z_3D} \\ A_{22} = \frac{Z_1+Z_2C-Z_3E}{Z_4+Z_2B-Z_3D} \end{cases} \tag{8}$$

and

$$\begin{cases} B = \frac{Z_2Z_4-Z_3(Z_1+R+\mathrm{j}Z_{\rm TL}\tan\theta_{\rm TL})}{(Z_1+R+\mathrm{j}Z_{\rm TL}\tan\theta_{\rm TL})^2-Z_4^2} \\ C = \frac{Z_3Z_4-Z_2(Z_1+R+\mathrm{j}Z_{\rm TL}\tan\theta_{\rm TL})}{(Z_1+R+\mathrm{j}Z_{\rm TL}\tan\theta_{\rm TL})^2-Z_4^2} \\ D = \frac{Z_2}{Z_1+R+\mathrm{j}Z_{\rm TL}\tan\theta_{\rm TL}} + \frac{Z_4B}{Z_1+R+\mathrm{j}Z_{\rm TL}\tan\theta_{\rm TL}} \\ E = \frac{Z_3}{Z_1+R+\mathrm{j}Z_{\rm TL}\tan\theta_{\rm TL}} + \frac{Z_4C}{Z_1+R+\mathrm{j}Z_{\rm TL}\tan\theta_{\rm TL}} \end{cases} \tag{9}$$

Based on the transformation relationship between A- and S-matrices, the S-parameters of the equivalent circuit can be expressed in terms of the A-parameters as

$$\begin{cases} S_{11} = \frac{A_{11}Z_0+A_{12}-A_{21}Z_0^2-A_{22}Z_0}{A_{11}Z_0+A_{12}+A_{21}Z_0^2+A_{22}Z_0} \\ S_{21} = \frac{2Z_0}{A_{11}Z_0+A_{12}+A_{21}Z_0^2+A_{22}Z_0} \end{cases} \tag{10}$$

To illustrate the validity and reliability of the derived formulae, Fig. 6 shows the comparison of theoretical calculation and simulation results. It can be seen that theoretical calculations and simulations are in agreement. The $|S_{11}|$ of the absorption network is less than -10 dB from 2 to 5 GHz, and the absorption network has a wideband out-of-band absorption function and frequency selectivity. Therefore, this absorption network can be cascaded with the filtering antenna to achieve wideband reflectionless filtering characteristics.

3.3. Analysis of Proposed Antenna

Figure 7 compares the simulated $|S_{11}|$ of the filtering antenna (i.e., Ant. III shown in Fig. 2) and the proposed antenna. It can be seen that the filtering antenna only has good impedance

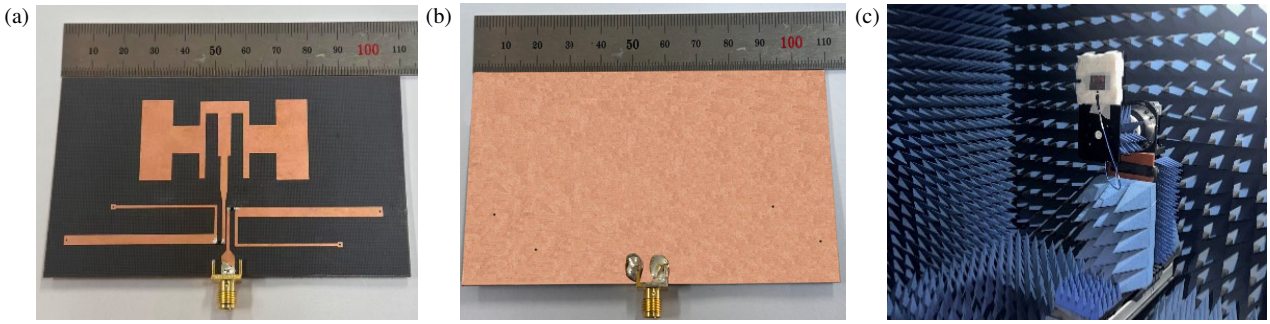

FIGURE 9. Photographs of the antenna prototype. (a) Top view. (b) Bottom view. (c) Testing environment.

TABLE 2. Performance comparisons with previous designs.

References	f_0 (GHz)	Substrate Layer	Gain (dBi)	Suppression Level (dB)	Reflectionless Bandwidth (%)	Size ($\lambda_g \times \lambda_g$)
[3]	2.3	3	5.2	> 13	N.A.	0.80×0.75
[7]	3.5	3	9.5	> 7.5	N.A.	1.17×1.17
[9]	5.8	1	7.3	> 17	25.9	0.77×0.77
[10]	6.8	3	9.0	> 29	34	0.71×0.71
[11]	5.5	2	6.0	> 15	32.3	0.81×0.72
[12]	32.5	3	6.0	> 15.5	15	0.65×0.54
[13]	2.7	1	4.8	> 7	19.7	1.03×0.71
This work	3.5	1	5.8	> 14.5	63.5	1.28×0.76

matching near the center frequency of 3.5 GHz. After cascading the absorption network, the proposed antenna has achieved wideband reflectionless filtering characteristics.

The most important parameter affecting the reflectionless performance of the proposed antenna is the length of the short-circuited transmission lines. As shown in Fig. 8, when L_e is increased from 42.22 mm to 42.82 mm, the impedance matching of the proposed reflectionless filtering antenna becomes better near 3.62 GHz, but the impedance matching near 3.4 GHz and the stopband suppression near 2.9 GHz become worse. Therefore, after comprehensive consideration, the value of L_e is selected as 42.52 mm.

4. RESULTS AND DISCUSSION

Figures 9(a) and 9(b) show photos of the antenna prototype. The $|S_{11}|$ is measured using an Agilent N5230A vector network analyzer, and the realized gain and radiation patterns are measured in a far-field anechoic chamber shown in Fig. 9(c).

The curves of simulated and measured $|S_{11}|$ and realized gain at the direction of the $+z$ axis are shown in Fig. 10. The measured -10-dB reflectionless bandwidth is 63.5% from 2.56 to 4.94 GHz. The measured peak gain is 5.8 dBi. Outside the passband, the measured two radiation nulls are located at 3.02 and 3.91 GHz, and the measured lower and upper stopband suppression levels are 18.1 and 14.5 dB, respectively. The simulated and measured radiation patterns of the E-plane and H-plane at the center frequency of 3.5 GHz are shown in Figs. 11(a) and 11(b), respectively. The measured cross-polarization level of the E-plane is less than -15 dB, and that of the H-plane is less than -7 dB. The cross-polarization level in the H-plane increases due to the unwanted higher-order modes at higher operating frequencies [14]. Fig. 12 shows the radiation efficiency versus frequency for the proposed filtering antenna. It is observed that the radiation efficiency at the center frequency of 3.5 GHz is about 73.7%. Table 2 shows the comparison of the proposed antenna with the published designs. As shown in Table 2, the proposed antenna has a wider reflectionless bandwidth and a moderate level of out-of-band suppression with

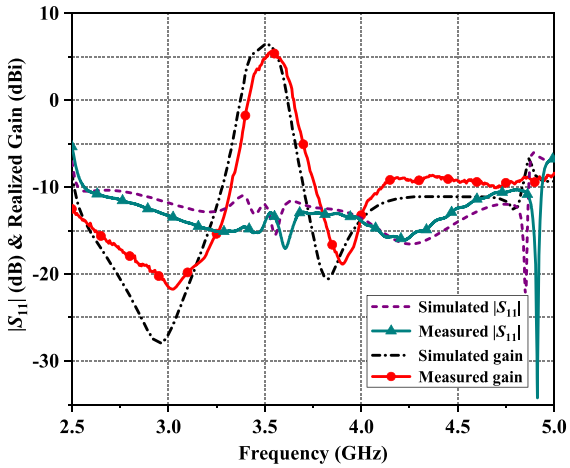

FIGURE 10. Simulation and measurement of $|S_{11}|$ and realized gain.

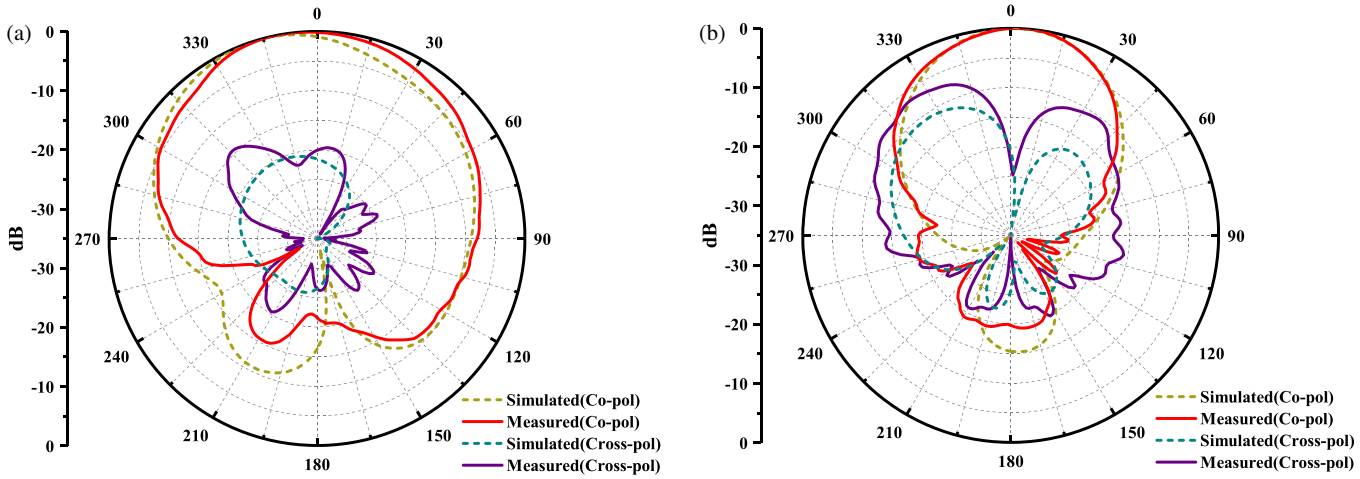

FIGURE 11. Simulation and measurement of normalized radiation pattern at 3.5 GHz. (a) E-plane. (b) H-plane.

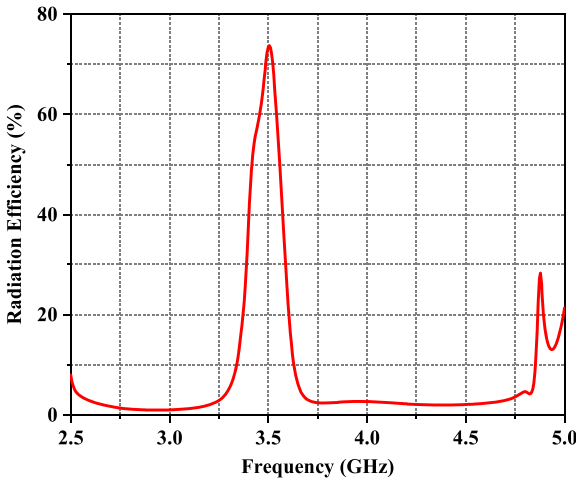

FIGURE 12. Simulated radiation efficiency of the proposed filtering antenna.

fewer substrate layers. However, due to the cascading of the absorption network and filtering antenna, the size of the proposed antenna becomes larger.

5. CONCLUSION

This paper presents a novel wideband reflectionless filtering patch antenna. Two radiation nulls are realized by an E-shape radiator and two T-shape radiators, respectively. By simply cascading the absorption network and filtering antenna, not only the design is greatly facilitated, but the proposed antenna also obtains out-of-band absorption capability and good out-of-band suppression. Through the fabrication and measurement of the reflectionless filtering patch antenna, the results show that wide out-of-band reflectionless bandwidth and good filtering performance are achieved. Owing to the out-of-band reflectionless characteristics of the antenna, this design effectively solves the influence of the out-of-band reflection signal of the filtering antenna on the stability of the power amplifier. So the proposed reflectionless filtering patch antenna has extensive application prospects in short-range communication systems [15].

ACKNOWLEDGEMENT

This work was supported by the National Natural Science Foundation of China (No. 52471371 and No. 61871417), the Liaoning Revitalization Talents Program (No. XLYC2007024), and the Basic Research Project of the Department of Education of Liaoning Province for Universities (No. LJ212410151023).

REFERENCES

[1] Jiang, Z. H. and D. H. Werner, "A compact, wideband circularly polarized co-designed filtering antenna and its application for wearable devices with low SAR," *IEEE Transactions on Antennas and Propagation*, Vol. 63, No. 9, 3808–3818, Sep. 2015.

[2] Deng, J., S. Hou, L. Zhao, and L. Guo, "A reconfigurable filtering antenna with integrated bandpass filters for UWB/WLAN applications," *IEEE Transactions on Antennas and Propagation*, Vol. 66, No. 1, 401–404, Jan. 2018.

[3] Zhang, B. and Q. Xue, "Filtering antenna with high selectivity using multiple coupling paths from source/load to resonators," *IEEE Transactions on Antennas and Propagation*, Vol. 66, No. 8, 4320–4325, Aug. 2018.

[4] Cheng, G., J. Zhou, L. Yang, X. Wu, and Z. Huang, "A stacked circularly polarized filtering antenna with crossed slot," *IEEE Antennas and Wireless Propagation Letters*, Vol. 22, No. 12, 2935–2939, Dec. 2023.

[5] Liu, G., P. F. Hu, G. D. Su, and Y. M. Pan, "Bandwidth and gain enhancement of a single-layer filtering patch antenna using reshaped TM mode," *IEEE Antennas and Wireless Propagation Letters*, Vol. 23, No. 1, 314–318, Jan. 2024.

[6] Chen, B.-J., X.-S. Yang, and B.-Z. Wang, "A compact high-selectivity wideband filtering antenna with multipath coupling structure," *IEEE Antennas and Wireless Propagation Letters*, Vol. 21, No. 8, 1654–1658, Aug. 2022.

[7] Yuan, H., F.-C. Chen, and Q.-X. Chu, "A wideband and high gain dual-polarized filtering antenna based on multiple patches," *IEEE Transactions on Antennas and Propagation*, Vol. 70, No. 10, 9843–9848, Oct. 2022.

[8] Wang, T., N. Yan, M. Tian, Y. Luo, and K. Ma, "A low-cost high-gain filtering patch antenna with enhanced frequency selectivity based on SISL for 5G application," *IEEE Antennas and Wireless Propagation Letters*, Vol. 21, No. 9, 1772–1776, Sep. 2022.

[9] Liu, Y.-T., K. W. Leung, and N. Yang, "Compact absorptive filtering patch antenna," *IEEE Transactions on Antennas and Propagation*, Vol. 68, No. 2, 633–642, Feb. 2020.

[10] Paul, V. and K. Dhwaj, "A reflectionless circularly polarized high gain microstrip filtering antenna with wideband response," *IEEE Transactions on Antennas and Propagation*, Vol. 72, No. 6, 5384–5389, Jun. 2024.

[11] Li, J.-F., C.-X. Mao, D.-L. Wu, L.-H. Ye, and G. Zhang, "A dual-beam wideband filtering patch antenna with absorptive band-edge radiation nulls," *IEEE Transactions on Antennas and Propagation*, Vol. 69, No. 12, 8926–8931, Dec. 2021.

[12] Fang, Z., J. Zhang, L. Gao, H. Chen, X. Yang, J. Liu, W. Li, and X. Cai, "Absorptive filtering packaging antenna design based on through-glass vias," *IEEE Transactions on Components, Packaging and Manufacturing Technology*, Vol. 13, No. 11, 1817–1824, Nov. 2023.

[13] Wang, S., F. Fan, R. Gómez-García, L. Yang, Y. Li, S.-W. Wong, and G. Zhang, "A planar absorptive-branch-loaded quasi-Yagi antenna with filtering capability and flat gain," *IEEE Antennas and Wireless Propagation Letters*, Vol. 20, No. 9, 1626–1630, Sep. 2021.

[14] Chen, Z. N. and M. Y. W. Chia, "Broad-band suspended probe-fed plate antenna with low cross-polarization levels," *IEEE Transactions on Antennas and Propagation*, Vol. 51, No. 2, 345–347, Feb. 2003.

[15] Leonardi, O., M. G. Pavone, G. Sorbello, A. F. Morabito, and T. Isernia, "Compact single-layer circularly polarized antenna for short-range communication systems," *Microwave and Optical Technology Letters*, Vol. 56, No. 8, 1843–1846, Aug. 2014.